3924–3933 *Nucleic Acids Research, 2009, Vol. 37, No. 12* *Published online 28 April 2009*
doi:10.1093/nar/gkp266

Highly efficient incorporation of the fluorescent nucleotide analogs tC and tC^{O} by Klenow fragment

Peter Sandin[1], Gudrun Stengel[2,*], Thomas Ljungdahl[1], Karl Börjesson[1], Bertil Macao[3] and L. Marcus Wilhelmsson[1,*]

[1]Department of Chemical and Biological Engineering/Physical Chemistry, Chalmers University of Technology, S-41296 Gothenburg, Sweden, [2]Department of Chemistry and Biochemistry, University of Colorado, Boulder, CO 80309-0215, USA and [3]Department of Medical Biochemistry, University of Gothenburg, PO Box 440, S-405 30 Gothenburg, Sweden

Received March 6, 2009; Revised April 9, 2009; Accepted April 9, 2009

ABSTRACT

Studies of the mechanisms by which DNA polymerases select the correct nucleotide frequently employ fluorescently labeled DNA to monitor conformational rearrangements of the polymerase–DNA complex in response to incoming nucleotides. For this purpose, fluorescent base analogs play an increasingly important role because they interfere less with the DNA–protein interaction than do tethered fluorophores. Here we report the incorporation of the 5′-triphosphates of two exceptionally bright cytosine analogs, 1,3-diaza-2-oxo-phenothiazine (tC) and its oxo-homolog, 1,3-diaza-2-oxo-phenoxazine (tC^{O}), into DNA by the Klenow fragment. Both nucleotide analogs are polymerized with slightly higher efficiency opposite guanine than cytosine triphosphate and are shown to bind with nanomolar affinity to the DNA polymerase active site, according to fluorescence anisotropy measurements. Using this method, we perform competitive binding experiments and show that they can be used to determine the dissociation constant of any given natural or unnatural nucleotide. The results demonstrate that the active site of the Klenow fragment is flexible enough to tolerate base pairs that are size-expanded in the major groove. In addition, the possibility to enzymatically polymerize a fluorescent nucleotide with high efficiency complements the tool box of biophysical probes available to study DNA replication.

INTRODUCTION

Fluorescent nucleobase analogs have been used in biophysical studies of nucleic acid structure and dynamics, DNA–protein interactions and the mechanism of DNA replication and repair for 30 years. Equally important, they are promising alternatives to tethered fluorophores in biotechnological applications, such as real-time quantitative PCR and fluorescence in situ hybridization [reviewed in Asseline (1)] and as sensors for single nucleotide polymorphisms (2–11) and enzyme activity (12–16). The prominent features that distinguish fluorescent base analogs from tethered dyes (i.e. a conventional dye is tethered to the nucleobase via a flexible linker, frequently to C-5 of cytosine) are their small size, their ability to base stack and potentially H-bond with the canonical bases as well as their minimal perturbation to the natural properties of the DNA duplex. Although dye-tethered nucleotides can be readily incorporated by DNA polymerases (17,18), fluorescent base analogs have the advantage of being positioned at a defined site inside the DNA helix via their base stacking and H-bonding interactions. This is an important advantage over tethered dyes where the presence of the dye linker makes it impossible to predict the exact location of the dye, thus tarnishing distance measurements by fluorescence resonance energy transfer (FRET). In comparison to the conventional tethered dyes, the fluorescence emission of today's base analogs is less bright, more sensitive to the analog's microenvironment and less photostable (19). While the sensitivity to the surrounding makes them excellent probes for studies of base flipping dynamics (20–26), DNA structure (27–32), protein binding and nucleotide incorporation and excision

*To whom correspondence should be addressed. Tel: +46 31 7723051; Fax: +46 31 7723858; Email: marcus.wilhelmsson@chalmers.se
Correspondence may also be addressed to Gudrun Stengel. Tel: +1 303 4923591; Fax: +1 303 4925894; Email: gudrun.stengel@colorado.edu

The authors wish it to be known that, in their opinion, the first two authors should be regarded as joint First Authors.

(33–36), it severely limits the usefulness of base analogs in applications that rely on high and stable quantum yields, such as FRET and single molecule and ensemble fluorescence imaging.

Virtually all existing base analogs have a fluorescence quantum yield that is highly dependent on their surrounding, i.e. the identity of the neighboring bases and hybridization state. While some analogs exhibit high quantum yields in certain base contexts {see for example the pteridine 3-MI (37), and benzo[g]quinazoline-2,4-(1H,3H)-dione (38)}, 1,3-diaza-2-oxo-phenothiazine (tC) and 1,3-diaza-2-oxo-phenoxazine (tC^O) are the only known base analogs that have a high fluorescence quantum yield regardless of the surrounding base sequence. tC and tC^O were originally introduced as anti-sense probes with enhanced binding affinity for RNA by Lin *et al*. (39), and further characterized with regard to their fluorescence and structural properties in our laboratory (40–43). Both are cytosine analogs that retain the functional groups for Watson–Crick base pairing with guanine while an expanded ring system projects into the major groove of DNA. Previously, Kool and coworkers have introduced fluorescent base analogs that are size-expanded by inserting an additional benzene ring between C-1′ of ribose and the nucleobase, thus widening the helix diameter (10,44).

The absorption and emission spectra of tC and tC^O are shifted to longer wavelengths relative to the absorption of the canonical bases and aromatic amino acids (Figure 1). The quantum yields of tC and tC^O is ~0.2 in double helical structures and display only little base sequence dependence (40,41). NMR and circular dichroism (CD) spectra as well as fluorescence decay and anisotropy data suggest that the analogs are rigidly stacked in the DNA helix and that the overall B conformation of duplex DNA is preserved in their presence, making tC and tC^O valuable biophysical probes (41,42).

The standard method for the incorporation of base analogs is the polymerization of the corresponding phosphoramidites by means of automated solid-phase DNA synthesis. Among the reported fluorescent nucleoside analogs 2-aminopurine (45), thieno[3,4-d]pyrimidine (4) and the polycyclic hydrocarbon pyrene (46) have been converted into the corresponding nucleotides and tested as substrates in DNA polymerase reactions. The possibility to incorporate fluorophores site-specifically by DNA polymerases offers a convenient avenue for multi-labeling of PCR products. Besides this practical merit, studies of the enzymatic incorporation of nucleotide analogs provide valuable insights into the mechanism of correct nucleotide recognition by DNA polymerases. Not much attention has been paid to the incorporation of fluorescent base analogs, presumably because their shapes tend to deviate significantly from the canonical bases. However, size-expanded bases like tC and tC^O are particularly interesting because they can give insights into the flexibility and size of the polymerase active site, a parameter that is believed to be important for correct base discrimination (47).

In this work, we report the synthesis of the 5′-triphosphates of the tC and tC^O deoxyribonucleosides and their incorporation into DNA by the Klenow fragment of DNA polymerase I from *Escherichia coli*.

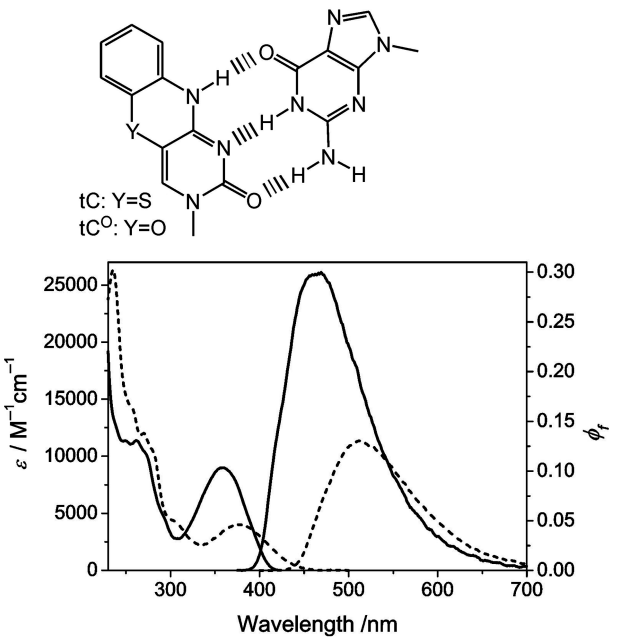

Figure 1. Chemical structure and base pairing pattern of the fluorescent base analogs tC and tC^O. Absorption and emission spectra of the free monomers of tC (dashed line) and tC^O (solid line). The fluorescence emission is normalized to represent the relative quantum yields.

Both analogs are identical to cytosine in their base pairing pattern but deviate significantly from cytosine in size. The objective of this work is to (i) find out if the analogs are site-specifically incorporated opposite G, (ii) determine the enzymatic efficiency of this process and (iii) demonstrate how the fluorescent properties of tC and tC^O can be employed to study nucleotide binding to DNA polymerases.

MATERIALS AND METHODS

Synthesis of 5′-triphosphate analogs

Materials. The pyridine used was dried by distillation from calcium hydride. Diisopropylethylamine (DIPEA) was distilled from ninhydrin/KOH. Phosphorus oxytrichloride and triethyl phosphate was distilled immediately prior to use. Total amount of 1 M triethylammonium acetate (TEAA) buffer was prepared by adding 2 mol triethylamine to 1 l of water, titrating with glacial acetic acid to pH 7.6 and diluting to 2 l. Total amount of 1.5 M triethylammonium bicarbonate (TEAB) buffer was prepared by adding 3 mol of triethylamine to 1.5 l water, bubbling carbon dioxide through the cooled suspension and diluting to 2 l once pH 7.8 was reached. Any changes in molarity resulting from evaporation of triethylamine during bubbling were ignored. Analytical high performance liquid chromatography (HPLC) was performed on a Waters system with Waters 600E system controller, Waters 717 (autosampler) and Waters Photodiode Array Detector, using a ReproSil-Pur C18-AQ, 5 μm, 250 × 4.6 mm column. The analyses were performed by ion-pairing chromatography with a gradient of 40% A + 60% B → 100% B in 15 min, where

A = 10 mM tetrabutylammonium bromide (TBABr), 10 mM KH_2PO_4, 2% ACN, pH 7.0 and B = 2:1 (10 mM TBABr, 100 mM KH_2PO_4, pH 7.0)/ACN.

The unphosphorylated nucleosides 3-(2-deoxy-β-D-ribofuranosyl)-1,3-diaza-2-oxo-phenothiazine (tC) and 3-(2-deoxy-β-D-ribofuranosyl)-1,3-diaza-2-oxo-phenoxazine (tC^O) were synthesized as described elsewhere (39,48). Phosphorylation of the 5′-hydroxy moiety was carried out according to Ludwig's procedure (49). In total 61 μmol of nucleoside was dried by co-evaporation twice with dry pyridine. After keeping under vacuum overnight triethyl phosphate (0.4 ml) was added and the suspension was cooled to −10°C. The nucleosides did not completely dissolve until later when the solution became slightly acidic from the liberation of HCl during the reaction progress. Phosphorus oxytrichloride (0.122 mmol, 11.4 μl, 2 equivalents) was added to the suspension and the reaction was allowed to run for 20 min at −10°C, after which the cooling bath was removed from the now clear yellow solution. After an additional 2 h, DIPEA (0.244 mmol, 42 μl, 4 equivalents) and tris(tetrabutylammonium) hydrogen pyrophosphate (275 mg, 0.305 mmol, 5 equivalents) dissolved in 0.25 ml DMF was added. After 10 min the reaction was quenched by the addition of TEAB (1.5 M, 1 ml). The quenched solution was diluted with water to reduce the ionic strength and was added to a short column of Sephadex DEAE-A25 equlibrated with 0.01 M TEAB. The product mixture was washed with 0.01 M TEAB to remove triethyl phosphate, unreacted starting material and other neutral compounds. The mixture of phosphorylated products and pyrophosphate was eluted with 1.5 M TEAB. The buffer was removed by lyophilization and the crude product was purified twice by RP-HPLC (C8, TEAA, pH 7.6; 5–15% ACN in 60 min), first using 0.1 M TEAA. The second run was performed using 0.01 M as this gave better separation and a highly pure product (>99% at 375 nm or 356 nm for tC and tC^O, respectively) but was too sensitive to run the crude reaction mixture in *3-(2-Deoxy-β-D-ribofuranosyl)-1,3-diaza-2-oxo-phenothiazine triphosphate (dtCTP)*. Obtained as a yellow hygroscopic solid in 14% yield. ^{31}P NMR (d6-DMSO) δ −18.6 (t, br), −6.5 (d, br), −5.3 (d, br); HRMS (FAB-) calculated for $[C_{15}H_{17}N_3O_{13}P_3S]^-$ 571.9695, found 571.9694. *3-(2-Deoxy-β-D-ribofuranosyl)-1,3-diaza-2-oxo-phenoxazine triphosphate (dtC^OTP)*. Obtained as an off-white hygroscopic solid in 15% yield. ^{31}P NMR (D_2O) δ −22.4 (t, br), −10.8 (d, br), −9.6 (d, br); HRMS (FAB-) calculated for $[C_{15}H_{17}N_3O_{14}P_3]^-$ 555.9923, found 555.9918.

Nucleotide incorporation assays

For single point measurements (Figures 2 and 3), reactions (30 μl) contained 2.0 μM prehybridized primer/template, 16.7 μM of the designated dNTPs, 11.6 nM Klenow fragment (Invitrogen), 50 mM Tris–HCl pH 8, 10 mM $MgCl_2$, and 50 mM NaCl. The base sequence of the primer/template construct was as follows:

5′-AAT CAC GGC GC
3′-TTA GTG CCG CG XTT GT with X being either A, G, T or C.

The reactions were stopped after 2 min by addition of 30 μl 80% formamide containing 50 mM EDTA. The extension products were separated by denaturing gel electrophoresis using a 20% polyacrylamide and 8 M urea gel and visualized by staining with SYBRgold (Invitrogen). The bands were quantified using a Typhoon fluorescence scanner (Molecular Dynamics).

Determination of kinetic parameters

DNA primers were 5′-^{32}P-labeled using T4 polynucleotide kinase (New England Biolab) and [γ-^{32}P]ATP. The labeled primer was gel-purified and annealed to the four different template strands. All kinetic data were determined under steady-state conditions following the method by Goodman *et al*. (50). Reactions (10 μl) typically contained 350 pM Klenow fragment 3′ → 5′ exo$^-$ (New England Biolab), 1 μM primer/template and between 0.05 and 10 μM dNTP (analog). Reactions were stopped after 1 min of incubation at 37°C by quenching with 10 μl 80% formamide containing 50 mM EDTA. Under these conditions, primer extension was below 20% for all reactions. Products were separated using 20% polyacrylamide and 8 M urea gels and imaged using a Typhoon phosphorimager (Molecular Dynamics). The amount of extended primer was quantified using ImageQuant 5.1 Software (Molecular Dynamics). The parameters K_M and V_{max} were obtained by plotting the amount of extended primer versus dNTP concentration and subsequent nonlinear curve fitting using the Michaelis–Menten equation.

Steady-state fluorescence anisotropy measurements

Measurements were carried out using a Quantamaster Fluorimeter in L-format equipped with motorized polarizers (Photon technology instruments). dtCTP and dtC^OTP were excited at 387 nm and 364 nm, respectively, and the fluorescence emission was monitored at 498 nm and 453 nm, respectively. All excitation and emission slits were set to 10 nm and the temperature was 25°C. Fluorescence anisotropy values were calculated from an average of 20 sets of single point measurements of the intensities I_{VV}, I_{VH} and $G = I_{HV}/I_{HH}$ using the expression $r = (I_{VV} - GI_{VH})/(I_{VV} + 2GI_{VH})$. The two subscripts H and V indicate the orientation of the excitation and emission polarizers. For example, I_{HV} corresponds to horizontally polarized excitation and vertically polarized emission.

Samples contained 50 mM Tris–HCl pH 8, 10 mM $MgCl_2$, 50 mM NaCl, 5% glycerol, a fixed amount of dtCTP or dtC^OTP (between 75 and 250 nM depending on the experiment) and 10 μM primer/template. The primer/template construct was the same as in the primer extension experiments, except that the 3′-end of the primer was terminated by 2′,3′-dideoxy-cytosine to prevent actual nucleotide incorporation. The total sample volume was 60 μl. In experiments designed to measure the dissociation constant of dtCTP (or dtC^OTP) (Figure 4), the ternary KF–DNA_n–dNTP complex was formed by gradually increasing the Klenow concentration in the sample. To this end, 1 μl portions of a concentrated Klenow solution (1.5 μM) were added to the sample and the fluorescence

anisotropy was recorded after each addition. In competition experiments (Figure 5), 250 or 125 nM fluorescent nucleotide analog was complexed with 283 nM of Klenow fragment and 10 μM primer/template (templating base was G) in a total volume of 60 μl. Under these conditions, most of the fluorescent nucleotides are bound in the ternary KF–DNA_n–dNTP complex, giving rise to high fluorescence anisotropy values. Subsequently, 1 μl portions of concentrated dCTP solutions were added to displace the fluorescent nucleotide from the ternary complex. The release of fluorescent nucleotide from the ternary complex resulted in the described decrease in fluorescence anisotropy.

RESULTS AND DISCUSSION

Single nucleotide extension assays

To test the ability of the Klenow fragment (KF) of *E. coli* DNA polymerase I to accept the 5′-triphosphate derivatives of the tC and tC^O nucleosides (dtCTP and dtC^OTP) as substrates, we performed primer extension assays with dCTP, dtCTP or dtC^OTP using template sequences in which the templating base (referred to as +1 position) was either A, G, T or C (Figure 2a). The extension products were separated by denaturing gel electrophoresis and visualized by staining with SYBRgold. Under the given reaction conditions the primer was readily elongated by dCTP, dtCTP and dtC^OTP when the templating base was G (Figure 2a). The total amount of extended primer was comparable for dCTP, dtCTP and dtC^OTP incorporation, suggesting that KF incorporated the cytidine nucleotide analogs as well as the natural substrate dCTP. The high efficiency is surprising in light of the large size of the resulting tC:G base pair. Previously, we observed that the KF readily incorporates dGTP opposite tC, forming a G:tC base pair (34). These results indicate that KF does not use interactions with the major groove to decide whether to polymerize a nucleotide or not.

Two other details are noteworthy. First, although KF did not misincorporate dtCTP when T was at the +1 position, a second band indicative of primer extension by two dtCMP is visible (Figure 2a) when T was at the +2 position and G was at the +1 position. The same trend for double incorporation was observed for both nucleotide analogs in the competitive primer extension assays where the nucleotide concentration was higher (Figure 3). This means the ability of the enzyme to distinguish between right and wrong substrate diminishes after addition of the analogs to the 3′-end of the primer, presumably due to strong hydrophobic interactions between the 3′-tC/tC^O and the incoming dtCTP/dtC^OTP. An alternative explanation would be that the analogs promote dislocation mutagenesis, i.e. slipping of the primer strand. Second, both nucleotide analogs, but dtC^OTP to a much larger extent, were incorporated opposite A (Figure 2a). Since H-bonding seems to be more relevant than base pair size in the case of tC and tC^O incorporation, this finding suggests that the electronic character of the nitrogen at N^4 (using the pyrimidine numbering system) is important for correct base pairing. It is not surprising that both the replacement of the primary amine of cytosine by a secondary amine and the attachment of an additional aromatic ring alter the electronic character of the N^4 nitrogen. Indeed, we recently reported that a DNA oligonucleotide containing a tC^O: A mismatch is significantly more stable than the corresponding duplex with a tC^O:T or tC^O:C mismatch (51). Moreover, the emission spectrum of the duplex with the tC^O:A mismatch exhibited a characteristic fine structure that may point towards firmer base stacking, a change in the polarity of the surroundings, a wobble A^+: C base pair resulting from the protonation of adenine

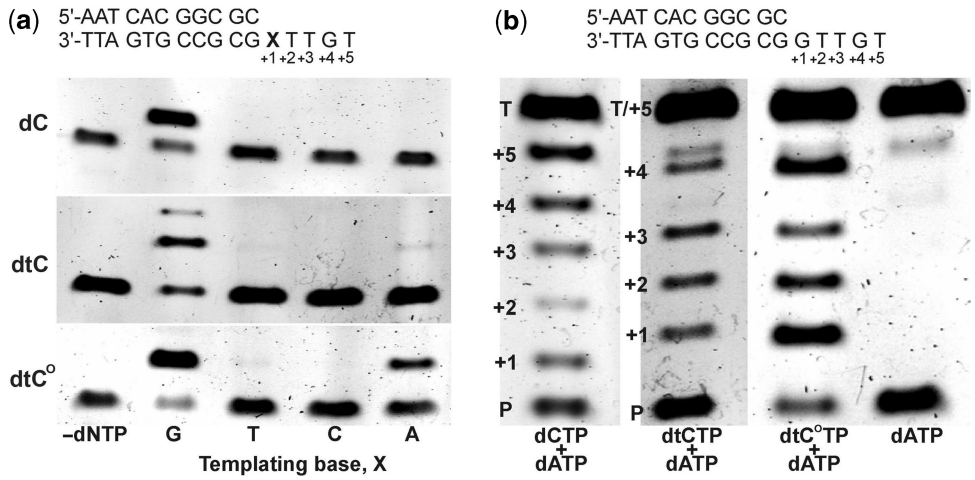

Figure 2. Incorporation of fluorescent nucleotide analogs by Klenow fragment. (**a**) Incorporation of dCTP (top), dtCTP (middle) and dtC^OTP (bottom) into the depicted primer/template with the templating base X being G, T, C or A. For primer extension, 16.7 μM nucleotide was reacted with 2 μM primer/template in the presence of 11.6 nM Klenow fragment. The reaction was stopped after 2 min by addition of formaldehyde and 50 mM EDTA. Control reactions without nucleotides are shown in the left lane. (**b**) Read-through assays of triphosphates dCTP (first lane), dtCTP (second lane) and dtC^OTP (third lane). The assay conditions were identical to (a) except that 16.7 μM of each nucleotide was added. Primer extension in the presence of dATP only (fourth lane). DNA strands were visualized by staining with SYBRgold.

at N-1 or hydrogen tautomerisation from the nitrogen at N^4 (pyrimidine numbering) to N-3 of tC^O.

Read through assays

Many unnatural nucleotide analogs, such as 1-deazapurine or 4-aminobenzimidazole (52) act as chain terminators, which limits their usefulness in biotechnological and medical applications. To test if KF can insert dtCTP and dtC^OTP in the presence of other nucleotides and produce a complete copy of the template strand, we repeated the primer extension assay above in the presence of dATP and either dCTP or one of the analog triphosphates. The sequence of the template overhang was 3′-GTTGT, requiring the incorporation of two base analogs relatively close together. The reaction containing dCTP produced primer strands extended by 1–5 bases (Figure 2b). The appearance of aborted products is expected since the reaction was stopped after only 2 min. Note that the template strand contained a minor impurity (template −1) that shows as a faint band at +5 (Figure 2b). In the reactions containing dtCTP and dtC^OTP, KF clearly inserted 1–4 bases. However, due to our staining method and the lower electrophoretic mobility of the analog-containing DNA strands, the band corresponding to the +5 extension product might comigrate with the template strand and may be indiscernible. To clarify if DNA polymerization is affected upstream of tC or tC^O, we repeated the read through assays using a primer/template with a 15-base overhang (data not shown). KF clearly polymerized 13 bases onto to the primer strand after inserting tC and tC^O at the +1 position, which is well beyond the distance where upstream effects are expected. Thus, tC and tC^O do not act as chain terminators.

Competitive primer extension assays

Next, we performed competitive primer extension assays, thereby exploiting the fact that primers extended by tC and tC^O migrate more slowly in the gel than primer strands containing C. Using the template with X = G, we varied the mole fraction of dCTP stepwise from 0% to 100% and compared the fraction of the primer elongated by either dtCTP (or dtC^OTP) or dCTP (Figure 3). If KF inserted the analogs with the same efficiency as C, the primer should be extended to equal extents by the analog and C at a dCTP mole fraction of 0.5. However, equal extension of the primer strands was observed at dCTP mole fractions of 0.75 and 0.8 for competition with dtCTP and dtC^OTP, respectively. Thus, KF prefers to polymerize the cytosine analogs over dCTP opposite G without being inhibited by the presence of the nucleotide analogs.

Steady-state kinetic parameters

To quantify the ability of KF to incorporate the analogs, we determined the Michaelis–Menten kinetic parameters K_M and V_{max} for nucleotide incorporation opposite G. The kinetic parameters were derived from single nucleotide insertion assays at varying dNTP concentrations (Table 1). The apparent efficiency (V_{max}/K_M) for dtCTP and dtC^OTP insertion was five and two times larger than for dCTP insertion opposite G, respectively, which agrees with the preference for the unnatural substrates we observed in our competitive extension assay (see above). A comparison of the V_{max} and K_M values reveals that the larger efficiency for analog incorporation is due to smaller K_M values for the analogs. Several studies have shown that the replacement of C with tC and tC^O increases the melting temperature of duplex DNA on average by 3°C, which is likely caused by stronger π–π stacking interactions with the neighboring bases due to the additional benzene ring (40,42). Hydrophobic interactions between the incoming nucleotide analog and the 3′-terminal base in the primer strand, together with the possibility of forming H-bonds, may drive the facile incorporation of the analog triphosphates.

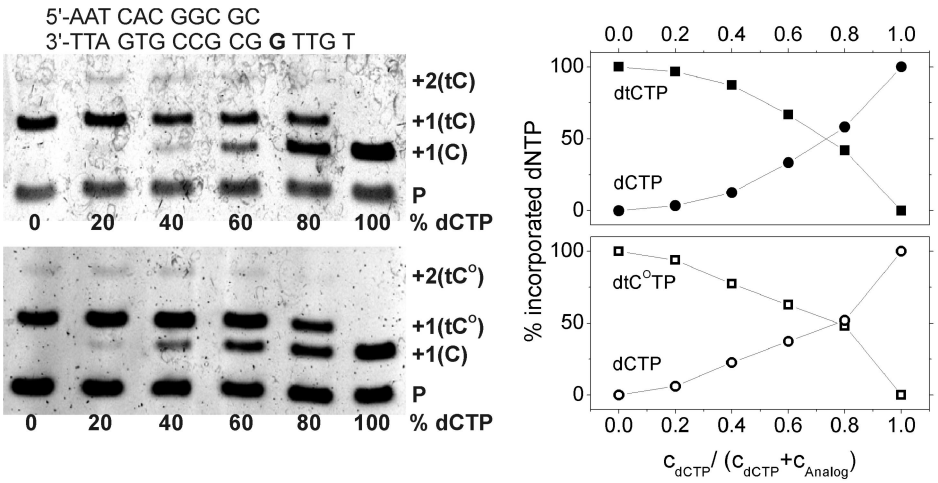

Figure 3. Competitive elongation experiments. Primer extension was performed in the presence of dCTP and dtCTP (top, left column) or dCTP and dtC^OTP (bottom left column) at different mixing ratios. The concentration of dCTP is given below the gels and the corresponding nucleotide analog concentration is 100% – (% dCTP). The products were analyzed by gel electrophoresis and the product bands stained with SYBRgold. The reaction conditions were like in Figure 2 with a total nucleotide concentration of 83.4 μM. The panel on the right displays the percentage of primer that was elongated by dtCTP (top) or by dtC^OTP (bottom) upon varying the mole fraction of dCTP.

Table 1. Steady-state kinetic parameters for the polymerization of nucleotide analogs opposite G

5′-AATCACGGCGC 3′-TTAGTGCCGCG**G**TTGT	K_M (μM)	V_{max} (%/min)	V_{max}/K_M (%/min M)	Discrimination[a]
+dCTP	0.41 (0.17)	8.4 (3.5)	20.5	1
+dtCTP	0.021 (0.03)	5.4 (1.4)	257.1	0.08
+dtC^{0}TP	0.16 (0.06)	8.4 (3.0)	52.5	0.39

[a]V_{max}/K_M for dCTP incorporation divided by V_{max}/K_M for analog incorporation.
The K_M and V_{max} values are given as an average of three independent measurements and the error is given in parenthesis.

Steady-state fluorescence anisotropy experiments

For protein–substrate complexes with slow substrate turn-over and fast dissociation of the protein and the reaction products, K_M is a good measure for the substrate affinity. However, in a polymerase reaction, the dissociation of the polymerase from the extended DNA primer can become rate-limiting. As a consequence, the reaction depletes of polymerase bound to unextended primer and no productive ternary polymerase–DNA–dNTP can stably exist. In this situation, K_M is fairly unrelated to the substrate affinity and therefore it is desirable to have an independent method for measuring substrate affinity. Here, we demonstrate how the fluorescence anisotropy of the nucleotide analogs can be used to measure the dissociation constant, K_D, of the ternary KF–DNA$_n$–dNTP complex according to the equilibrium:

$$KF - DNA_n{-}dNTP \rightleftharpoons KF - DNA_n + dNTP$$

with,

$$K_D = \frac{[KF - DNA_n][dNTP]}{[KF - DNA_n{-}dNTP]}$$

Fluorescence anisotropy measures the rotational dynamics of a molecule during the lifetime of the excited state. While small fluorophores perform fast, unhindered rotations in aqueous media, their rotational dynamics slows significantly when bound to a high molecular mass compound like a protein or DNA. The change in rotational dynamics results in an increase in fluorescence anisotropy. There are two main advantages of using tC and tC^O for this kind of studies. First, we have shown that the tricyclic fluorescent base analogs have a base-flipping rate that will not interfere with the signal measured in fluorescence anisotropy (38,40). Generally base analogs such as 2-aminopurine have increased base flipping dynamics that will affect the measured anisotropy and thus complicate interpretation. Second, tC and tC^O are on average the brightest base analogs available (e.g. ~25–50 times brighter than 2-AP) which means a significant increase in accuracy. Here we exploit these advantages to obtain additional information on the binding of dtCTP and dtC^{O}TP to the binary KF–DNA$_n$ complex.

The nucleotide analog was mixed with a 40-fold excess of primer/template (X = G), the primer of which was 3′-terminated with a 2′,3′-dideoxy-CMP to prevent nucleotide incorporation. The fluorescence anisotropy of both nucleotide analogs was about $r = 0.025$ in the unbound state. Upon addition of KF we observed a gradual increase in the fluorescence anisotropy of the nucleotide analogs (Figure 4). When KF was in small excess over the nucleotide analogs, the anisotropy approached $r = 0.25$ and $r = 0.2$ for dtCTP and dtC^{O}TP, respectively. Note that these values do not represent the anisotropy at saturated binding since we probed only a narrow concentration range of KF. The K_D for the formation of the binary KF–DNA$_n$ complex is 5 nM according to published data (53). Under our assay

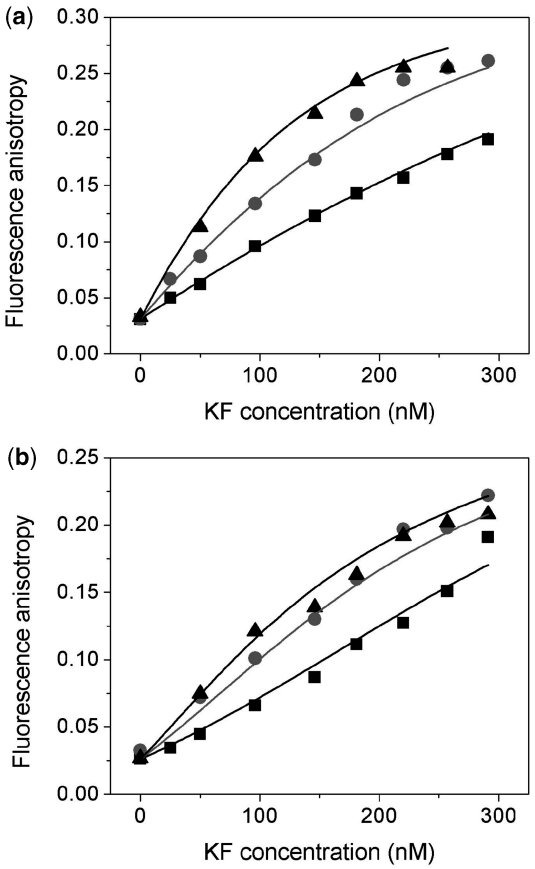

Figure 4. Formation of the ternary KF–DNA–dNTP complex probed by steady-state fluorescence anisotropy. (**a**) In three separate experiments, 125 nM (black triangles), 250 nM (gray circles) and 500 nM (black squares) dtCTP was incubated with increasing amounts of KF in the presence of 10 μM primer/template (X = G). In all binding experiments, the 3′-end of the primer was terminated with a 2′,3′-dideoxy-cytosine. (**b**) The same experiments were carried out using 75 nM (black triangles), 125 nM (gray circles) and 250 nM (black squares) dtC^{O}TP. The affinity curves resulting from the best fits (see text) are shown as solid curves.

conditions ([DNA] = 10 μM), KF is trapped in the binary KF–DNA_n complex and hence, the increase in anisotropy reports the formation of the ternary KF–DNA_n–dNTP complex. According to X-ray crystal structures of Klentaq, a structural homolog of KF, the enzyme exists in a closed and an open conformational state (54). In the closed state, the incoming nucleotide stacks with the 3′-terminal primer base and is held in place opposite the templating base via H-bonds. The closed conformation is likely to restrict the rotational freedom of the nucleotide. The observed increase in fluorescence anisotropy suggests a shift of the conformational equilibrium towards the closed state. Interestingly, an increase in anisotropy was not observed with a primer/template exhibiting A as templating base (data not shown).

The fluorescence anisotropy, r, is represented as the sum of the contributions from free and bound nucleotide probe, each weighted according to their contribution to the total fluorescence intensity:

$$r = \frac{(1 - f_b)r_f + xf_b r_b}{1 - f_b + xf_b} \quad \mathbf{1}$$

where f_b is the fraction of bound probe, r_f is the anisotropy of the free probe, r_b is the anisotropy of bound probe, and x is the intensity of bound probe/intensity of free probe.

For the simple 1:1 association of nucleotide probe [dtCTP in Equation (2)] with binary KF–DNA complex, f_b is given by (55):

$$f_b = \frac{([\mathrm{KF \cdot DNA}_n] + [\mathrm{dtCTP}] + K_D) - \sqrt{([\mathrm{KF \cdot DNA}_n] + [\mathrm{dtCTP}] + K_D)^2 - 4[\mathrm{KF \cdot DNA}_n][\mathrm{dtCTP}]}}{2[\mathrm{dtCTP}]} \quad \mathbf{2}$$

Note that [dtCTP] refers to the total nucleotide concentration. Similarly, [KF·DNA_n] denotes the total amount of KF used in the assay (this concentration is assumed to equal the concentration of binary KF–DNA_n owing to the large excess of DNA, see above). Inserting Equation (2) into Equation (1) yields an expression that was used to obtain K_D from the anisotropy curves displayed in Figure 4 by means of non-linear curve fitting. The analysis was performed globally, which means the three binding curves obtained at different nucleotide concentrations were fitted simultaneously to yield shared results for x, r_b and K_D. For dtCTP, we found $r_b = 0.35$ and $K_D = 64 \pm 15$ nM; the binding curves for dtC^{O}TP, were well described by $r_b = 0.35$ and $K_D = 60 \pm 21$ nM. The difference between dtCTP and dtC^{O}TP in curve shape despite the similar K_D values originates from the fact that the fluorescence emission of dtCTP is slightly enhanced upon protein binding (measured to $x = 1.20$, inset Figure 5a), whereas the emission of dtC^{O}TP is quenched (measured to $x = 0.48$, inset Figure 5b). The fit yields theoretical values of $x = 1.26$ and $x = 0.39$ for dtCTP and dtC^{O}TP, respectively, in good agreement with the experimentally determined values.

To make sure that we observe binding of the nucleotide analogs to the active site of KF and that the increase in anisotropy is not a consequence of unspecific hydrophobic

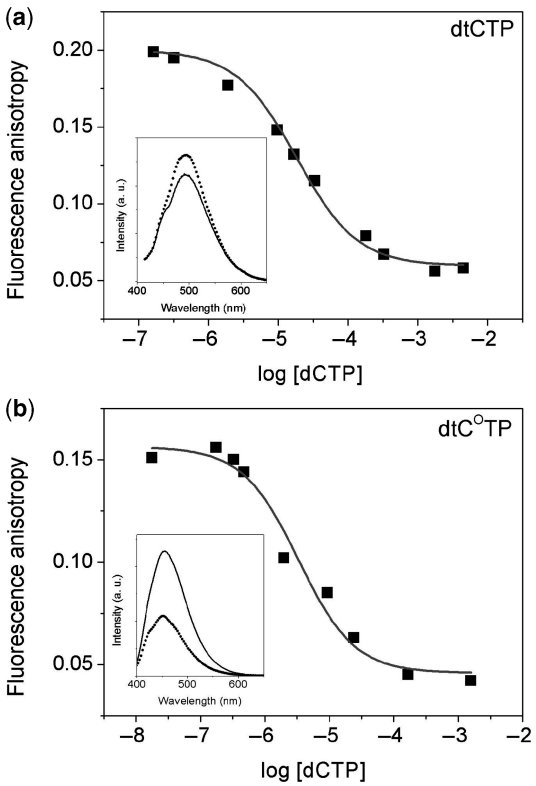

Figure 5. Competitive binding curves. The samples contained 10 μM primer/template (X = G), 203 nM KF and 250 nM dtCTP (**a**) or 250 nM dtC^{O}TP (**b**). The stepwise addition of dCTP (black squares) replaces the fluorescent nucleoside triphosphates in the ternary complexes. Insets: Effect of protein binding on the fluorescence emission of dtCTP (inset in a) and dtC^{O}TP (inset in b). Total 125 nM nucleotide analog were incubated with 284 nM Klenow fragment and 10 μM primer/template (X = G) until the fluorescence remained stable. Spectra of the free nucleotide analogs are shown as black lines and spectra of the nucleotides in complex with KF are shown as black dots.

interactions, we performed control measurements in the absence of DNA and with the three other primer/template constructs (with X = A, T, C) (data not shown). In these experiments, we observed only a very small increase in anisotropy. Thus, the high anisotropy is specific for the cognate ternary complex where the nucleotide analog is stacked opposite G. One should note that the affinity of the nucleotide analogs for KF alone or in complex with a mismatched template might be too low to yield a substantial amount of complex in the studied range of KF concentrations. In any case, the control experiments exclude unspecific protein-nucleotide interactions as possible cause for the observed fluorescence anisotropy increase. According to literature data, K_D for binding of the correct dNTP in the ternary KF–DNA–dNTP complex ranges between 4 and 20 μM depending on the base context (56). This indicates that dtCTP and dtC^{O}TP bind ~100 times more tightly showing that base pair size is not limiting but affords additional stabilization, most likely by hydrophobic stacking interactions. One should keep in mind though that the dissociation constants for the natural dNTPs have been determined

using a different method, which may introduce some degree of inaccuracy.

Next, we set up competitive binding experiments to prove that dCTP and the cytidine analogs bind to the same binding pocket. The nucleotide analog was incubated with a nearly equimolar amount of KF and a 40-fold excess of primer/template (X = G), resulting in ternary complex formation and the corresponding high anisotropy value. When dCTP was added, the anisotropy dropped gradually as the analog was replaced by dCTP (Figure 5). If the fluorescent ligand and the unlabeled competitor both bind reversibly to the same binding site, binding at equilibrium is described by the following sigmoidal curve (57):

$$y = bottom + \frac{(top - bottom)}{1 + 10^{\log[dCTP] - \log IC_{50}}} \quad \mathbf{3}$$

with IC_{50} being the competitor concentration that reduces the fluorescence signal by 50%.

Using Equation (3), we derived IC_{50} values of 18.6 and 3.4 μM when 250 nM dtCTP or dtC^{O}TP were complexed with 203 nM KF. Thus, a large excess of dCTP is necessary to replace the nucleotide analogs. The difference in the IC50 values for tC and tC^{O} implies that the ternary complex with dtCTP was approximately five times more stable. A similar trend was seen in the K_M for incorporation of dtCTP opposite G. However, we cannot exclude the possibility that the dtC^{O}TP competition curve is slightly shifted towards lower IC50 values because of the fluorescence quenching of tC^{O} upon KF binding. Since the brighter species, which is the free dtC^{O}TP, has a larger contribution to the overall fluorescence anisotropy, the anisotropy should drop more rapidly as dtC^{O}TP is released from the protein. In total, the competitive binding experiments confirm specific and reversible binding of the nucleotides to the active site and KF. Moreover, assays of this kind would be perfectly suited to measure the K_D of any dNTP through the competition with a fluorescent nucleotide analog.

CONCLUSIONS

In summary, we show the highly efficient incorporation of the fluorescent cytidine analogs dtCTP and dtC^{O}TP by the Klenow fragment. To the best of our knowledge, this is the first report of the insertion of a size-expanded base that is more efficient than the insertion of the corresponding natural base. The high efficiency is afforded by low K_D and K_M values for the binding of the nucleotide analogs to the DNA polymerase together with nearly unaffected V_{max}. Our results suggest that the active site of the KF is flexible enough to tolerate the additional mass added by tC and tC^{O} in the major groove, which is in good agreement with the facile incorporation of other bulky nucleotide analogs (17–18,58). However, the misincorporation of the nucleotide analogs opposite A hint towards a loss of selectivity. This aspect is under investigation and will be presented in a forthcoming publication. The results also show that it is possible to increase the affinity of nucleotide binding by means of a suitable ring extension while retaining the H-bonding capacity of the natural base pair. Moreover, a fluorescent nucleotide that can be enzymatically inserted into DNA is a highly interesting addition to the biophysical probes available to study DNA replication.

FUNDING

Swedish Research Council, the European Commission's Sixth Framework Programme (Project reference AMNA, contract no. 013 575); NIH grant (GM54 194) to Robert D. Kuchta (University of Colorado at Boulder). Funding for open access charge: Swedish Research Council.

Conflict of interest statement. None declared.

REFERENCES

1. Asseline,U. (2006) Development and applications of fluorescent oligonucleotides. *Curr. Org. Chem.*, **10**, 491–518.
2. Cekan,P. and Sigurdsson,S.T. (2008) Single base interrogation by a fluorescent nucleotide: each of the four DNA bases identified by fluorescence spectroscopy. *Chem. Commun.*, **29**, 3393–3395.
3. Tanaka,K. and Okamoto,A. (2008) Design of a pyrene-containing fluorescence probe for labeling of RNA poly(A) tracts. *Bioorg. Med. Chem.*, **16**, 400–404.
4. Srivatsan,S.G., Weizman,H. and Tor,Y. (2008) A highly fluorescent nucleoside analog based on thieno[3,4-d] pyrimidine senses mismatched pairing. *Org. Biomol. Chem.*, **6**, 1334–1338.
5. Srivatsan,S.G. and Tor,Y. (2007) Fluorescent pyrimidine ribonucleotide: Synthesis, enzymatic incorporation, and utilization. *J. Am. Chem. Soc.*, **129**, 2044–2053.
6. Socher,E., Jarikote,D.V., Knoll,A., Roglin,L., Burmeister,J. and Seitz,O. (2008) FIT probes: Peptide nucleic acid probes with a fluorescent base surrogate enable real-time DNA quantification and single nucleotide polymorphism discovery. *Anal. Biochem.*, **375**, 318–330.
7. Saito,Y., Hanawa,K., Kawasaki,N., Bag,S.S. and Saito,I. (2006) Acridone-labeled base-discriminating fluorescence (BDF) nucleoside: Synthesis and their photophysical properties. *Chem. Lett.*, **35**, 1182–1183.
8. Okamoto,A., Tainaka,K. and Saito,I. (2003) Clear distinction of purine bases on the complementary strand by a fluorescence change of a novel fluorescent nucleoside. *J. Am. Chem. Soc.*, **125**, 4972–4973.
9. Mizuta,M., Seio,K., Miyata,K. and Sekine,M. (2007) Fluorescent pyrimidopyrimidoindole nucleosides: Control of photophysical characterizations by substituent effects. *J. Org. Chem.*, **72**, 5046–5055.
10. Krueger,A.T. and Kool,E.T. (2008) Fluorescence of size-expanded DNA bases: reporting on DNA sequence and structure with an unnatural genetic set. *J. Am. Chem. Soc.*, **130**, 3989–3999.
11. Ikeda,S., Kubota,T., Kino,K. and Okamoto,A. (2008) Sequence dependence of fluorescence emission and quenching of doubly thiazole orange labeled DNA: effective design of a hybridization-sensitive probe. *Bioconjugate Chem.*, **19**, 1719–1725.
12. Moser,A.M., Patel,M., Yoo,H., Balis,F.M. and Hawkins,M.E. (2000) Real-time fluorescence assay for O-6-alkylguanine-DNA alkyltransferase. *Anal. Biochem.*, **281**, 216–222.
13. Stivers,J.T., Pankiewicz,K.W. and Watanabe,K.A. (1999) Kinetic mechanism of damage site recognition and uracil flipping by Escherichia coli uracil DNA glycosylase. *Biochemistry.*, **38**, 952–963.
14. Otto,M.R., Bloom,L.B., Goodman,M.F. and Beechem,J.M. (1998) Stopped-flow fluorescence study of precatalytic primer strand base-unstacking transitions in the exonuclease cleft of bacteriophage T4 DNA polymerase. *Biochemistry.*, **37**, 10156–10163.
15. Hawkins,M.E., Pfleiderer,W., Mazumder,A., Pommier,Y.G. and Falls,F.M. (1995) Incorporation of a fluorescent guanosine analog into oligonucleotides and its application to a real-time assay for the

HIV-1 integrase 3′-processing reaction. *Nucleic Acids Res.*, **23**, 2872–2880.
16. Raney,K.D., Sowers,L.C., Millar,D.P. and Benkovic,S.J. (1994) A fluorescence-based assay for monitoring helicase activity. *Proc. Natl Acad. Sci. USA*, **91**, 6644–6648.
17. Giller,G., Tasara,T., Angerer,B., Muhlegger,K., Amacker,M. and Winter,H. (2003) Incorporation of reporter molecule-labeled nucleotides by DNA polymerases. I. Chemical synthesis of various reporter group-labeled 2′-deoxyribonucleoside-5′-triphosphates. *Nucleic Acids Res.*, **31**, 2630–2635.
18. Tasara,T., Angerer,B., Damond,M., Winter,H., Dorhofer,S., Hubscher,U. and Amacker,M. (2003) Incorporation of reporter molecule-labeled nucleotides by DNA polymerases. II. High-density labeling of natural DNA. *Nucleic Acids Res.*, **31**, 2636–2646.
19. Rist,M.J. and Marino,J.P. (2002) Fluorescent nucleotide base analogs as probes of nucleic acid structure, dynamics and interactions. *Curr. Org. Chem.*, **6**, 775–793.
20. Yang,K.S., Matsika,S. and Stanley,R.J. (2007) 6MAP, a fluorescent adenine analogue, is a probe of base flipping by DNA photolyase. *J. Phys. Chem. B.*, **111**, 10615–10625.
21. Chandrashekaran,S., Manjunatha,U.H. and Nagaraja,V. (2004) KpnI restriction endonuclease and methyltransferase exhibit contrasting mode of sequence recognition. *Nucleic Acids Res.*, **32**, 3148–3155.
22. Gowher,H. and Jeltsch,A. (2000) Molecular enzymology of the EcoRV DNA-(adenine-N(6))-methyltransferase: kinetics of DNA binding and bending, kinetic mechanism and linear diffusion of the enzyme on DNA. *J. Mol. Biol.*, **303**, 93–110.
23. Pues,H., Bleimling,N., Holz,B., Wolcke,J. and Weinhold,E. (1999) Functional roles of the conserved aromatic amino acid residues at position 108 (motif IV) and position 196 (motif VIII) in base flipping and catalysis by the N6-adenine DNA methyltransferase from Thermus aquaticus. *Biochemistry*, **38**, 1426–1434.
24. Mernagh,D.R., Taylor,I.A. and Kneale,G.G. (1998) Interaction of the type I methyltransferase M.EcoR1241 with modified DNA substrates: sequence discrimination and base flipping. *Biochem. J.*, **336**, 719–725.
25. Holz,B., Klimasauskas,S., Serva,S. and Weinhold,E. (1998) 2-Aminopurine as a fluorescent probe for DNA base flipping by methyltransferases. *Nucleic Acids Res.*, **26**, 1076–1083.
26. Allan,B.W., Beechem,J.M., Lindstrom,W.M. and Reich,N.O. (1998) Direct real time observation of base flipping by the EcoRI DNA methyltransferase. *J. Biol. Chem.*, **273**, 2368–2373.
27. Kenfack,C.A., Piemont,E., Ben Gaied,N., Burger,A. and Mely,Y. (2008) Time-resolved fluorescent properties of 8-vinyl-deoxyadenosine and 2-amino-deoxyribosylpurine exhibit different sensitivity to their opposite base in duplexes. *J. Phys. Chem. B.*, **112**, 9736–9745.
28. Lee,B.J., Barch,M., Castner,E.W., Volker,J. and Breslauer,K.J. (2007) Structure and dynamics in DNA looped domains: CAG triplet repeat sequence dynamics probed by 2-aminopurine fluorescence. *Biochemistry*, **46**, 10756–10766.
29. Raghavan,S.C., Houston,S., Hegde,B.G., Langen,R., Haworth,I.S. and Lieber,M.R. (2004) Stability and strand asymmetry in the non-B DNA structure at the bcl-2 major breakpoint region. *J. Biol. Chem.*, **279**, 46213–46225.
30. Huizenga,D.E. and Szostak,J.W. (1995) A DNA aptamer that binds adenosine and ATP. *Biochemistry*, **34**, 656–665.
31. Guest,C.R., Hochstrasser,R.A., Sowers,L.C. and Millar,D.P. (1991) Dynamics of mismatched base-pairs in DNA. *Biochemistry*, **30**, 3271–3279.
32. Nordlund,T.M., Andersson,S., Nilsson,L., Rigler,R., Gräslund,A. and McLaughlin,L.W. (1989) Structure and dynamics of a fluorescent DNA oligomer containing the EcorI recognition sequence – fluorescence, molecular-dynamics, and NMR-studies. *Biochemistry*, **28**, 9095–9103.
33. Zhang,H., Cao,W., Zakharova,E., Konigsberg,W. and De la Cruz,E.M. (2007) Fluorescence of 2-aminopurine reveals rapid conformational changes in the RB69 DNA polymerase-primer/template complexes upon binding and incorporation of matched deoxynucleoside triphosphates. *Nucleic Acids Res.*, **35**, 6052–6062.
34. Stengel,G., Gill,J.P., Sandin,P., Wilhelmsson,L.M., Albinsson,B., Nordén,B. and Millar,D. (2007) Conformational dynamics of DNA polymerase probed with a novel fluorescent DNA base analogue. *Biochemistry*, **46**, 12289–12297.
35. DeLucia,A.M., Grindley,N.D.F. and Joyce,C.M. (2007) Conformational changes during normal and error-prone incorporation of nucleotides by a y-family DNA polymerase detected by 2-aminopurine fluorescence. *Biochemistry*, **46**, 10790–10803.
36. Purohit,V., Grindley,N.D.F. and Joyce,C.M. (2003) Use of 2-aminopurine fluorescence to examine conformational changes during nucleotide incorporation by DNA polymerase I (Klenow fragment). *Biochemistry*, **42**, 10200–10211.
37. Hawkins,M.E., Pfleiderer,W., Balis,F.M., Porter,D. and Knutson,J.R. (1997) Fluorescence properties of pteridine nucleoside analogs as monomers and incorporated into oligonucleotides. *Anal. Biochem*, **244**, 86–95.
38. Godde,F., Toulmé,J.-J. and Moreau,S. (1998) Benzoquinazoline derivatives as substitutes for thymine in nucleic acid complexes. Use of fluorescence emission of benzo[g]quinazoline-2,4-(1H,3H)-dione in probing duplex and triplex formation. *Biochemistry*, **37**, 13765–13775.
39. Lin,K.Y., Jones,R.J. and Matteucci,M. (1995) Tricyclic 2′-deoxycytidine analogs – syntheses and incorporation into oligodeoxynucleotides which have enhanced binding to complementary RNA. *J. Am. Chem. Soc.*, **117**, 3873–3874.
40. Sandin,P., Börjesson,K., Li,H., Mårtensson,J., Brown,T., Wilhelmsson,L.M. and Albinsson,B. (2008) Characterization and use of an unprecedentedly bright and structurally non-perturbing fluorescent DNA base analogue. *Nucleic Acids Res.*, **36**, 157–167.
41. Sandin,P., Wilhelmsson,L.M., Lincoln,P., Powers,V.E.C., Brown,T. and Albinsson,B. (2005) Fluorescent properties of DNA base analogue tC upon incorporation into DNA – negligible influence of neighbouring bases on fluorescence quantum yield. *Nucleic Acids Res.*, **33**, 5019–5025.
42. Engman,K.C., Sandin,P., Osborne,S., Brown,T., Billeter,M., Lincoln,P., Nordén,B., Albinsson,B. and Wilhelmsson,L.M. (2004) DNA adopts normal B-form upon incorporation of highly fluorescent DNA base analogue tC: NMR structure and UV-Vis spectroscopy characterization. *Nucleic Acids Res.*, **32**, 5087–5095.
43. Wilhelmsson,L.M., Sandin,P., Holmén,A., Albinsson,B., Lincoln,P. and Nordén,B. (2003) Photophysical characterization of fluorescent DNA base analogue, tC. *J. Phys. Chem. B.*, **107**, 9094–9101.
44. Chelliserrykattil,J., Lu,H., Lee,A.H.F. and Kool,E.T. (2008) Polymerase amplification, cloning, and gene expression of benzo-homologues 'yDNA' base pairs. *Chem. Bio. Chem.*, **9**, 2976–2980.
45. Bloom,L.B., Otto,M.R., Beechem,J.M. and Goodman,M.F. (1993) Influence of 5′-nearest neighbors on the insertion kinetics of the fluorescent nucleotide analog 2-aminopurine by Klenow fragment. *Biochemistry*, **32**, 11247–11258.
46. Matray,T.J. and Kool,E.T. (1999) A specific partner for abasic damage in DNA. *Nature*, **399**, 704–708.
47. Kool,E.T. (2002) Active site tightness and substrate fit in DNA replication. *Annu. Rev. Biochem.*, **71**, 191–219.
48. Sandin,P., Lincoln,P., Brown,T. and Wilhelmsson,L.M. (2007) Synthesis and oligonucleotide incorporation of fluorescent cytosine analogue tC: a promising nucleic acid probe. *Nature Protocols*, **2**, 615–623.
49. Ludwig,J. (1981) A new route to nucleoside 5′-triphosphates. *Acta Biochim. Biophys. Acad. Sci. Hung.*, **16**, 131–133.
50. Goodman,M.F., Creighton,S., Bloom,L.B. and Petruska,J. (1993) Biochemical basis of DNA-replication fidelity. *Crit. Rev. Biochem. Mol. Biol.*, **28**, 83–126.
51. Börjesson,K., Sandin,P. and Wilhelmsson,L.M. (2009) Nucleic acid structure and sequence probing using fluorescent base analogue tC^{O}. *Biophys. Chem.*, **139**, 24–28.
52. Beckman,J., Kincaid,K., Hocek,M., Spratt,T., Engels,J., Cosstick,R. and Kuchta,R.D. (2007) Human DNA polymerase alpha uses a combination of positive and negative selectivity to polymerize purine dNTPs with high fidelity. *Biochemistry*, **46**, 448–460.
53. Dahlberg,M.E. and Benkovic,S.J. (1991) Kinetic mechanism of DNA polymerase I (Klenow fragment): identification of a second conformational change and evaluation of the internal equilibrium constant. *Biochemistry*, **30**, 4835–4843.

54. Li,Y., Korolev,S. and Waksman,G. (1998) Crystal structures of open and closed forms of binary and tertnary complexes of the large fragment of Thermus aquaticus DNA polymerase I: structural basis for nucleotide incorporation. *EMBO J.*, **17**, 7514–7525.
55. Bailey,M.F., van der Schans,E.J.C. and Millar,D.P. (2004) Thermodynamic dissection of the polymerizing and editing modes of a DNA polymerase. *J. Mol. Biol.*, **336**, 673–693.
56. Eger,B.T., Kuchta,R.D., Carroll,S.S., Benkovic,P.A., Dahlberg,M.E., Joyce,C.M. and Benkovic,S.J. (1991) Mechanism of DNA-replication fidelity for 3 mutants of DNA-polymerase I: Klenow fragment KF(Exo+), KF(Pola5), and KF(Exo-). *Biochemistry*, **30**, 1441–1448.
57. Cheng,Y. and Prusoff,W.H. (1973) Relationship between inhibition constant (K1) and concentration of inhibitor which causes 50 per cent inhibition (I50) of an enzymatic-reaction. *Biochem. Pharmacol.*, **22**, 3099–3108.
58. Moran,S., Ren,R.X.F., Rumney,S. and Kool,E.T. (1997) Difluorotoluene, a nonpolar isostere for thymine, codes specifically and efficiently for adenine in DNA replication. *J. Am. Chem. Soc.*, **119**, 2056–2057.